The Application of Interface Elements to Dissimilar Meshes in Global/Local Analysis

John E. Schiermeier
Senior Development Engineer
The MacNeal–Schwendler Corporation
Los Angeles, California

Jerrold M. Housner
Jonathan B. Ransom
NASA Langley Research Center
Hampton, Virginia

Mohammad A. Aminpour
Applied Research Associates, Inc.
Hampton, Virginia

W. Jefferson Stroud
NASA Langley Research Center
Hampton, Virginia

The 1996 MSC World Users' Conference
Newport Beach, California
June 3–7, 1996

Abstract

When performing global/local analysis, the issue of connecting dissimilar meshes often arises, especially when refinement is performed. One method of connecting these dissimilar meshes is to use interface elements. In MSC/NASTRAN Version 69, interface elements have been implemented for the p–shell elements. This paper will discuss the elements and present examples.

1. Introduction

1.1. Applications

The problem of connecting dissimilar meshes at a common interface is a major one in finite element analysis. Such interfaces can result from a variety of sources, which can be divided into two categories: those generated by the analyst, and those generated by the analysis program.

Dissimilar meshes generated by the analyst can occur with global/local analysis, where part of the structure is modeled as the area of primary interest, in which detailed stress distributions are required, and part of the structure is modeled as the area of secondary interest, through which load paths are passed into the area of primary interest. Generally the area of primary interest has a finer mesh than the area of secondary interest, and therefore a transition area is required. Severe transitions generally produce elements that are heavily distorted, which can result in poor stresses and poor load transfer into the area of primary interest. An example of using interface elements to avoid such transitions is shown in Figure 1. Similarly, a patch of elements may be removed from the global model and replaced by a denser patch for local detail.

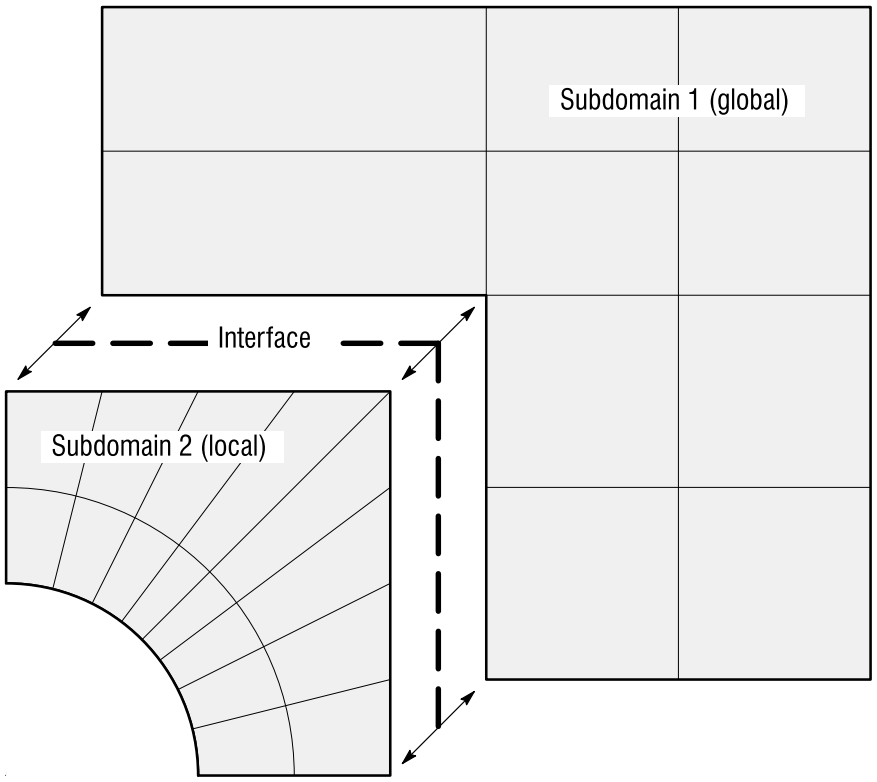

Figure 1: Example of Interface Elements (exploded view).

In large system problems, different analysts or even different organizations may have created different components of the model, such as the wing and the fuselage of an airplane. Unless they have carefully coordinated their efforts, the finite element meshes of the different components may not match, as otherwise required, at the interfaces.

Dissimilar meshes generated by the analysis program can arise with automeshers, which may be required to transition between large elements and small elements in a limited area. Many automeshers

generate tetrahedral meshes for solids, and distorted tetrahedra may be more susceptible to poor results. Automeshers are often used in conjunction with shape optimization procedures, where the shape changes are large enough to warrant remeshing. In these cases, it would be more efficient to remesh only the local part of the model and interface it with the rest, rather than remeshing the entire model. If the rest of the model has not been remeshed, then the associated parts of the stiffness matrix need not be recalculated, provided that the previous data has been saved.

In h–refinement, subdivided elements may be adjacent to undivided elements with no room for a transition area. Without some kind of interface element, the subdivision would have to be carried out to the model boundary or otherwise phased out.

1.2. Previous Methods

Much work has been done to resolve the element interface problem, with most of the efforts concentrating on moving the nodes or writing multi–point constraint (MPC) equations on the interfaces. The first approach, moving the nodes, must take into account the element distortions on both sides of the interface and provide the best redistribution according to some criteria. However, it is possible that one or both sides of the interface may be represented only by previously–generated stiffness matrices, in which case the nodes cannot be moved. The biggest restriction of moving nodes is that both sides of the interface must have the same number and type of elements. Therefore, this method is not practical for the general problem.

The second approach, using MPC equations, often is used for connecting elements of different types. For example, the midside node of a quadratic element may be constrained to move linearly with the vertex nodes in order to match an adjacent linear element, assuming that the vertex nodes for the two elements are coincident. Other MPC equations, such as splines, can handle more general cases. However, MPC equations by definition provide additional relationships for the existing degrees of freedom on the interface, and in the process reduce the number of independent degrees of freedom. If there are no degrees of freedom created, this could result in additional local stiffness or other non–physical effects in the model.

1.3. Current Method

The need and applications for reliable interface technology are great. NASA Langley Research Center has developed a method for analyzing plate and shell structures composed of two or more independently modeled substructures, based on a hybrid variational formulation with Lagrange multipliers, and applied it to global/local demonstration problems [1–4].

Under terms of a cooperative agreement between MSC and NASA [5], MSC is implementing this technology into MSC/NASTRAN for the p–shell elements along a geometric curve. This agreement is part of NASA's continuing effort to transfer technology into the mainstream of industry as an aid in developing competitiveness in the worldwide market.

2. Formulation

The formulation of the interface element, which is a hybrid variational formulation using Lagrange multipliers, is defined in summary as follows, using primarily the notation in [1]. It is repeated in more general form here to include the dynamic case. The complete details for the static case may be found in [1–3].

The displacement vector $\{v\}$ on the interface is defined in terms of the node and edge coefficients $\{q_s\}$, which are defined on the interface elements, and interpolation functions $[T]$, which is a matrix containing the functions for each field of the interface displacement vector:

$$\{v\} = [T]\{q_s\}$$

The displacement vector $\{u_j\}$ on each subdomain j is defined in terms of the node and edge coefficients $\{q_j\}$ and interpolation functions $[N_j]$, which is a matrix containing the functions for each field of the subdomain displacement vector:

$$\{u_j\} = [N_j]\{q_j\}$$

The Lagrange multiplier vector $\{\lambda_j\}$ on each subdomain j is defined in terms of the node and edge coefficients $\{\alpha_j\}$ and interpolation functions $[R_j]$, which is a matrix containing the functions for each field of the Lagrange multiplier vector:

$$\{\lambda_j\} = [R_j]\{\alpha_j\}$$

Defining the combined operator and material matrix $[B_j]$, the density ρ, and the surface tractions $\{t_j\}$; and considering the potential energy for all the subdomains j with the internal energy, inertial forces, and applied forces, and for the interface I with the Lagrange multipliers gives:

$$\Pi = \sum_j \left[\frac{1}{2} \int_\Omega u_j{}^T \; B_j \; u_j \; dA + \frac{1}{2} \int_\Omega u_j{}^T \; \rho_j \; \ddot{u}_j \; dA - \int_\Gamma u_j{}^T \; t \; ds + \int_I \lambda_j{}^T \; \left(v - u_j \right) \; ds \right]$$

where the inertial body forces:

$$F_j = - \rho_j \; \ddot{u}_j$$

have been multiplied by a factor of one half since they are proportional loads. Using the standard assumption of simple harmonic motion for the frequency ω:

$$\ddot{u}_j = - \omega^2 \; u_j$$

and expanding the vectors into their coefficients and interpolation functions gives:

$$\Pi = \sum_j \left[\frac{1}{2} \int_\Omega q_j{}^T \; N_j{}^T \; G_j \; N_j \; q_j \; dA - \frac{1}{2} \int_\Omega q_j{}^T \; N_j{}^T \; \rho_j \; \omega^2 \; N_j \; q_j \; dA - \int_\Gamma q_j{}^T \; N_j{}^T \; t_j \; ds \right.$$
$$\left. + \int_I \left(q_s{}^T \; T^T - q_j{}^T \; N_j{}^T \right) \; R_j \; \alpha_j \; ds \right]$$

Defining the matrices of interpolation functions:

$$M_j = - \int_I N_j{}^T \; R_j \; ds$$

$$G_j = \int_I T^T \; R_j \; ds$$

and substituting these, together with the standard definition of stiffness matrices $[k_j]$, mass matrices $[m_j]$, and load vectors $\{f_j\}$, into the potential energy gives:

$$\Pi = \sum_j \left[\frac{1}{2} q_j^T \; k_j \; q_j - \frac{1}{2} \omega^2 q_j^T \; m_j \; q_j - q_j^T \; f_j + \left(q_s^T \; G_j + q_j^T \; M_j \right) \alpha_j \right]$$

Partitioning the q into q^i, those node and edge coefficients on the interface, and q^o, those coefficients other than on the interface, gives:

$$\Pi = \sum_j \left\{ \frac{1}{2} \begin{bmatrix} q_j^{o\,T} & q_j^{i\,T} \end{bmatrix} \begin{bmatrix} k_j^{oo} & k_j^{oi} \\ k_j^{io} & k_j^{ii} \end{bmatrix} \begin{Bmatrix} q_j^o \\ q_j^i \end{Bmatrix} - \frac{1}{2} \omega^2 \begin{bmatrix} q_j^{o\,T} & q_j^{i\,T} \end{bmatrix} \begin{bmatrix} m_j^{oo} & m_j^{oi} \\ m_j^{io} & m_j^{ii} \end{bmatrix} \begin{Bmatrix} q_j^o \\ q_j^i \end{Bmatrix} \right.$$

$$\left. - \begin{bmatrix} q_j^{i\,T} & q_j^{o\,T} \end{bmatrix} \begin{Bmatrix} f_j^i \\ f_j^o \end{Bmatrix} + \left(\begin{bmatrix} q_s^T \end{bmatrix} \begin{bmatrix} G_j \end{bmatrix} + \begin{bmatrix} q_j^{i\,T} \end{bmatrix} \begin{bmatrix} M_j \end{bmatrix} \right) \{\alpha_j\} \right\}$$

Deriving the Euler equations by taking the variations of the potential energy with respect to the four groups of variables q_j^o, q_j^i, q_s, and α_j gives:

$$\frac{\partial \Pi}{\partial q_j^o} = \left(k_j^{oo} - \omega^2 \; m_j^{oo} \right) q_j^o + \left(k_j^{oi} - \omega^2 \; m_j^{oi} \right) q_j^i - f_j^o = 0$$

$$\frac{\partial \Pi}{\partial q_j^i} = \left(k_j^{io} - \omega^2 \; m_j^{io} \right) q_j^o + \left(k_j^{ii} - \omega^2 \; m_j^{ii} \right) q_j^i - f_j^i + M_j \; \alpha_j = 0$$

$$\frac{\partial \Pi}{\partial q_s} = \sum_j G_j \; \alpha_j = 0$$

$$\frac{\partial \Pi}{\partial \alpha_j} = G_j^T \; q_s + M_j^T \; q_j^i = 0$$

Each of the Euler equations has a physical interpretation. Writing the Euler equations in matrix form:

$$\left(\begin{bmatrix} k_j^{oo} & k_j^{oi} & \dots & 0 & 0 & \dots \\ k_j^{io} & k_j^{ii} & \dots & 0 & M_j & \dots \\ \vdots & \vdots & & \vdots & \vdots & \\ 0 & 0 & \dots & 0 & G_j & \dots \\ 0 & M_j^T & \dots & G_j^T & 0 & \dots \\ \vdots & \vdots & & \vdots & \vdots & \end{bmatrix} - \omega^2 \begin{bmatrix} m_j^{oo} & m_j^{oi} & \dots & 0 & 0 & \dots \\ m_j^{io} & m_j^{ii} & \dots & 0 & 0 & \dots \\ \vdots & \vdots & & \vdots & \vdots & \\ 0 & 0 & \dots & 0 & 0 & \dots \\ 0 & 0 & \dots & 0 & 0 & \dots \\ \vdots & \vdots & & \vdots & \vdots & \end{bmatrix} \right) \begin{Bmatrix} q_j^o \\ q_j^i \\ \vdots \\ q_s \\ \alpha_j \\ \vdots \end{Bmatrix} = \begin{Bmatrix} f_j^o \\ f_j^i \\ \vdots \\ 0 \\ 0 \\ \vdots \end{Bmatrix}$$

This system of equations is symmetric, but not positive definite. All of the interface terms $[M_j]$ and $[G_j]$ appear in the stiffness matrix, with none in the mass matrix. Had damping been included, which generally takes the form of a load proportional to the velocity, the result would have been similar.

3. Implementation

The addition of interface elements allows dissimilar meshes to be connected over a common geometric boundary, instead of using transition meshes or constraint conditions. Primary applications where the analyst specifies the interface elements manually include: facilitating global/local analysis, where a patch of elements may be removed from the global model and replaced by a denser patch for a local detail, without having to transition to the surrounding area; and connecting meshes built by different engineering organizations, such as a wing to the fuselage of an airplane. Primary applications where the interface elements could be generated automatically are related to: automeshers, which may be required to transition between large and small elements between mesh regions; and h–refinement, where subdivided elements may be adjacent to undivided elements without a transition area.

Three new bulk data entries, GMBNDC (Geometric Boundary – Curve), GMINTC (Geometric Interface – Curve), and PINTC (Properties of Geometric Interface – Curve), were implemented for specifying the curve interface elements. These entries define the boundaries of the subdomains, the interface elements, and the interface element properties, respectively. Detailed information on the input data is available in [6].

Currently there are three methods of defining the boundaries of p–shell elements on the boundary of a subdomain, as shown in Figure 2. For the curve interface, each boundary may be defined using the GMCURV with which the finite element edges are associated, the FEEDGEs defining the finite element edges, or in the most basic form, the GRIDs along the finite element edges.

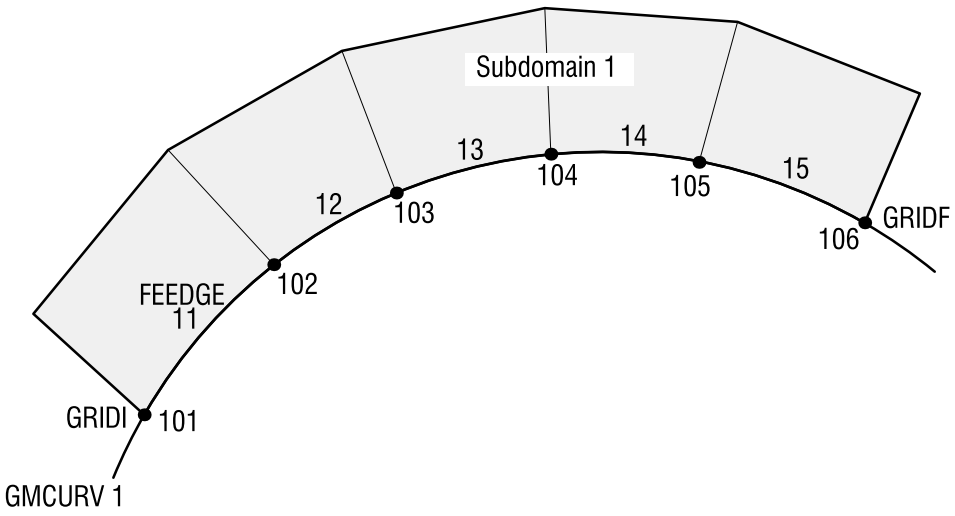

Figure 2: Geometric Boundary Definition.

Once the boundaries have been defined, they must be associated with the interface elements, as shown in Figure 3. This is accomplished by referencing the boundaries in the interface element definition.

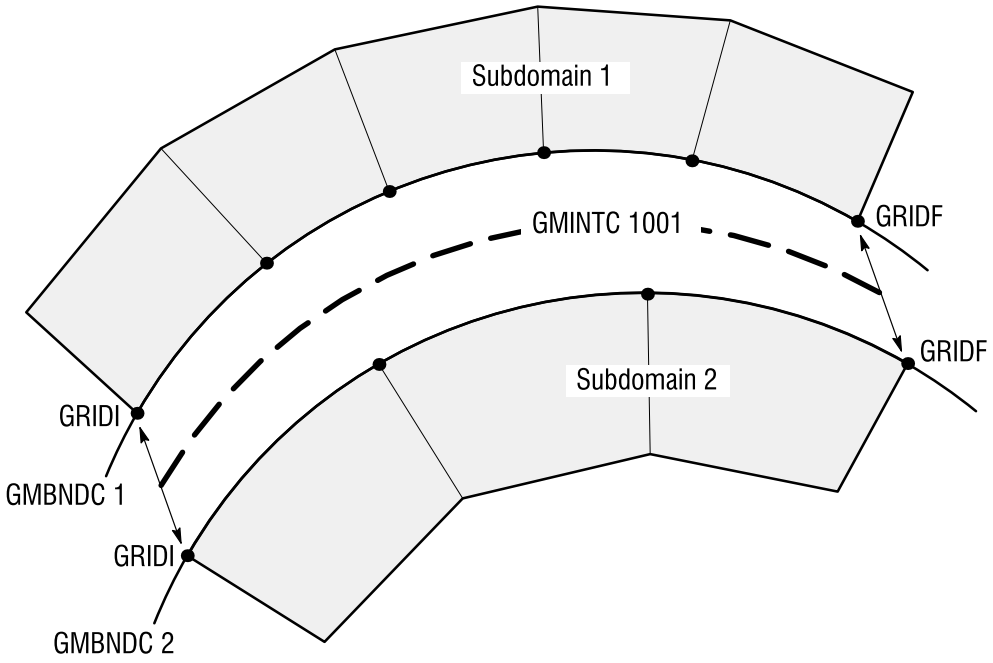

Figure 3: Interface Element Definition (exploded view).

Since the interface elements consist only of the differences in displacement components weighted by the Lagrange multipliers, there are no conventional element or material properties. The property bulk data entry specifies a tolerance for the interface elements, which defines the allowable distance between the boundaries of the subdomains.

4. Example Problems

Several sets of example problems were analyzed, in order to test the capabilities of the interface elements with various boundary configurations. The goal of the interface element is that it should not decrease the accuracy below that obtained using the less refined boundary with a conforming mesh. However, it will not increase the accuracy above that obtained using the more refined boundary with a conforming mesh. For example, if one boundary had two element edges and the other had three element edges at a given p–level, the accuracy with the interface elements should fall between a similar problem with two conforming two–edge boundaries and a similar problem with two conforming three–edge boundaries.

4.1. Cantilever Beam

The first set of example problems used a cantilever beam that had exact solutions at low p–levels. Three of the non–conforming configurations are shown in Figure 4.

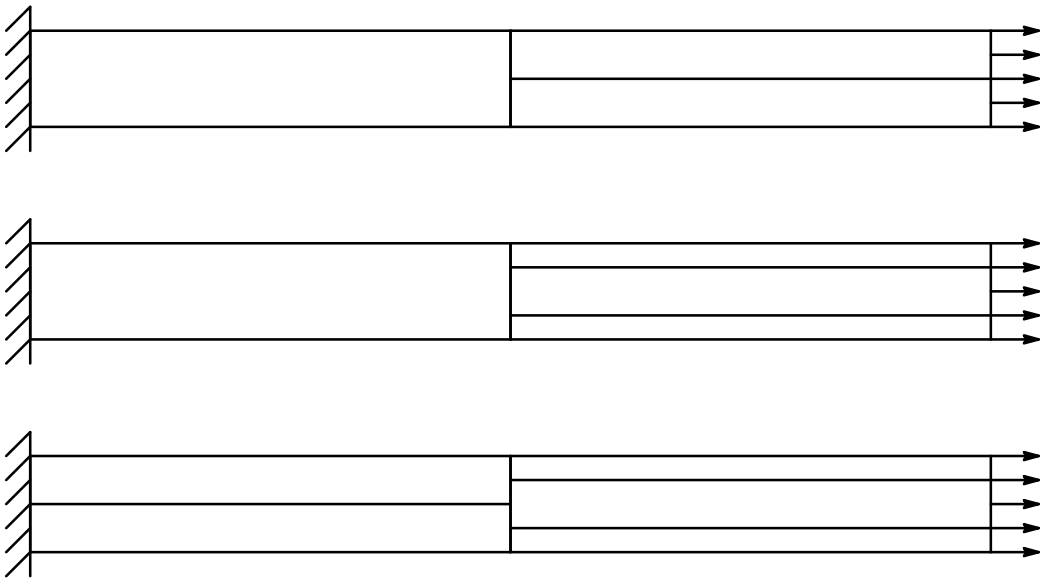

Figure 4: Cantilever Beam

Tension (exact at p=1), moment (exact at p=2), in–plane shear (exact at p=3), out–of–plane shear (exact at p=3), and torsion (not exact) load cases were analyzed. The von Mises stress contours at p=8 for all five of these cases with the two–element/three–element mesh are shown on the deformed shape in Figure 5. The data recovery mesh is used, rather than on the original p–element mesh, so that better resolution of the deformed shape and stress contours may be shown. (Note that there are no stress contours for the tension case, since it has uniform stress.)

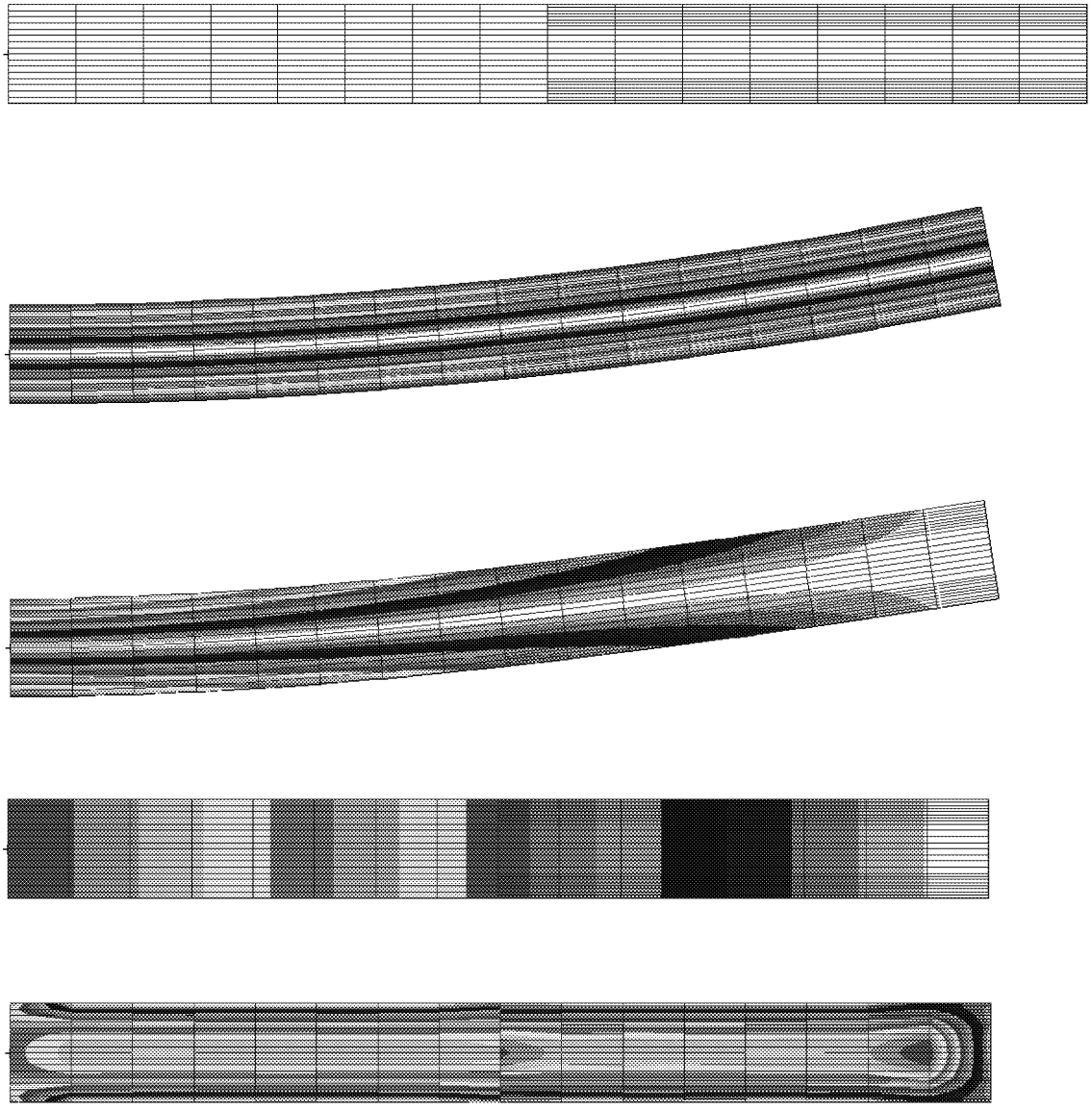

Figure 5: von Mises Stress Contours on Deformed Shape (p=8)

The normalized values of the external work at p=3 for the five load cases are listed in Table 1 for three conforming and three non–conforming meshes, all with interface elements. (Note that since the torsion case is not exact, the value for the three–element/three–element conforming mesh without interface elements at p=8 was used for normalization.) For the tension, moment, and two shear cases, the results were exact for all six meshes. For the torsion case, with the exception of the one–element/two–element mesh, the results were progressively better as additional elements were added, independently of whether the mesh was conforming or not.

Table 1: Normalized External Work (p=3)

mesh	tension	moment	shear (in–plane)	shear (out–plane)	torsion
one/one with interface	1.0000	1.0000	1.0000	1.0000	0.9875
one/two with interface	1.0000	1.0000	1.0000	1.0000	0.9866
one/three with interface	1.0000	1.0000	1.0000	1.0000	0.9897
two/two with interface	1.0000	1.0000	1.0000	1.0000	0.9902
two/three with interface	1.0000	1.0000	1.0000	1.0000	0.9919
three/three with interface	1.0000	1.0000	1.0000	1.0000	0.9951

The normalized values of the external work at p=8 for the five load cases are listed in Table 2 for the six meshes. For the tension, moment, and two shear cases, the results were again exact for all six meshes. This illustrates the stability of the interface elements as the p–level increases. For the torsion case, the results were progressively better as additional elements were added, independently of whether the mesh was conforming or not. The three–element/three–element mesh with interface elements gave exactly the same results as the same mesh without interface elements.

Table 2: Normalized External Work (p=8)

mesh	tension	moment	shear (in–plane)	shear (out–plane)	torsion
one/one with interface	1.0000	1.0000	1.0000	1.0000	0.9996
one/two with interface	1.0000	1.0000	1.0000	1.0000	0.9997
one/three with interface	1.0000	1.0000	1.0000	1.0000	0.9997
two/two with interface	1.0000	1.0000	1.0000	1.0000	0.9999
two/three with interface	1.0000	1.0000	1.0000	1.0000	0.9999
three/three with interface	1.0000	1.0000	1.0000	1.0000	1.0000

4.2. Scordelis–Lo Roof

The second set of example problems used the Scordelis–Lo roof [7], which includes curvature in the interface elements and both membrane and bending behavior in the shell elements. One of the configurations is shown in Figure 6. (Note that this particular mesh refinement is not the most advantageous, but is being used to illustrate the interface elements.)

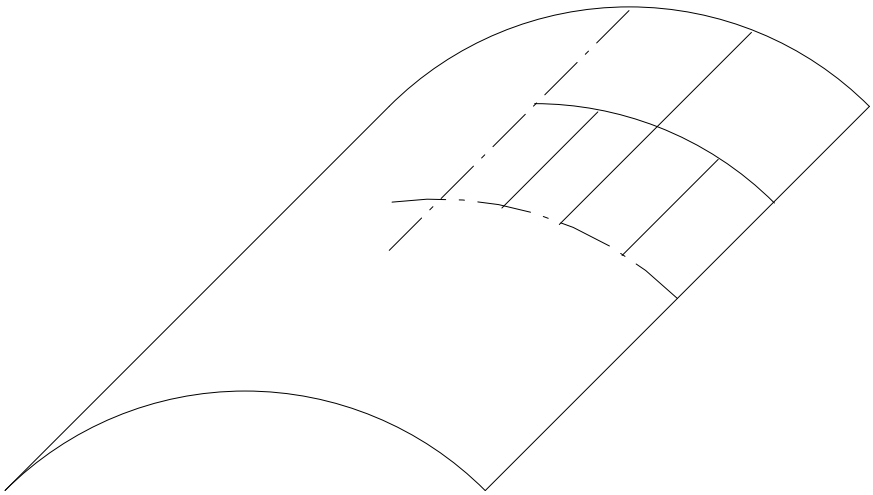

Figure 6: Scordelis–Lo Roof

The roof has simple supports on the curved edges and is loaded by its own weight. Using symmetry constraints, only a quarter of the model was analyzed. The vertical displacement contours for the two–element/four–element mesh are shown on the deformed shape in Figure 7. The contours are again shown on the data recovery mesh.

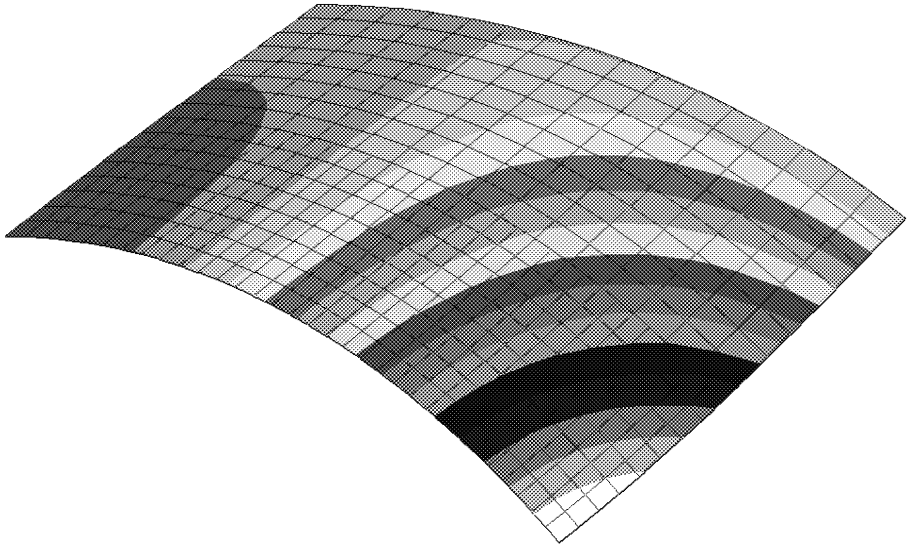

Figure 7: Vertical Displacement Contours on Deformed Shape (p=8)

The vertical displacements at the midside of the free edge at p=3 are listed in Table 3 for two conforming and two non–conforming meshes with interface elements and two conforming meshes without interface elements, which will serve as baselines. The value cited in [7] is –0.3086, with the notation that many elements converge to a lower value such as –0.3024. For the two conforming configurations, the meshes with and without interface elements match exactly. Of the displacements for the two non–conforming meshes, one falls within the range of the conforming configurations, whereas the other does not, but the solution at p=3 has not yet converged.

Table 3: Midside Vertical Displacement (p=3)

Mesh	Displacement
two/two without interface	–0.3176
two/two with interface	–0.3176
two/three with interface	–0.3162
two/four with interface	–0.3182
four/four with interface	–0.3195
four/four without interface	–0.3195

The vertical displacements at the midside of the free edge at p=8 are listed in Table 4 for the same four meshes with interface elements and two meshes without. For the two conforming configurations, the meshes with and without interface elements again match exactly. Of the displacements for the two non–conforming meshes, both fall within the range of the conforming configurations, creating a monotonic progression as elements are added, since the p=8 solution is closer to convergence.

Table 4: Midside Vertical Displacement (p=8)

Mesh	Displacement
two/two without interface	–0.3025
two/two with interface	–0.3025
two/three with interface	–0.3031
two/four with interface	–0.3034
four/four with interface	–0.3044
four/four without interface	–0.3044

4.3. Square Plate with Circular Hole

The third problem is a square plate with a circular hole, as shown in Figure 8. The hole is small enough relative to the plate that additional elements, though not necessary, greatly improve convergence. This example better illustrates how a global/local problem could be modelled, since the patch of elements around the hole could be replaced without modifying the mesh away from the hole.

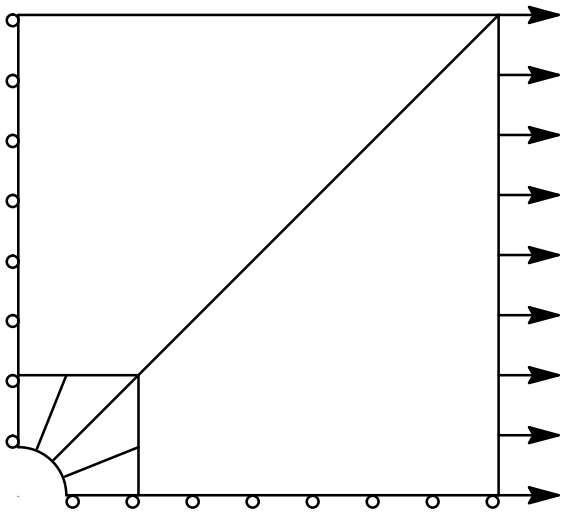

Figure 8: Square Plate with Circular Hole.

The square plate has a uniform tension load, so that the stress concentration factor at the hole may be calculated, and symmetry constraints. Two interface elements were used, since the interface contains a right angle. The horizontal stress contours for the four–element/two–element non–conforming mesh are shown on the deformed shape in Figure 9. The contours are again shown on the data recovery mesh.

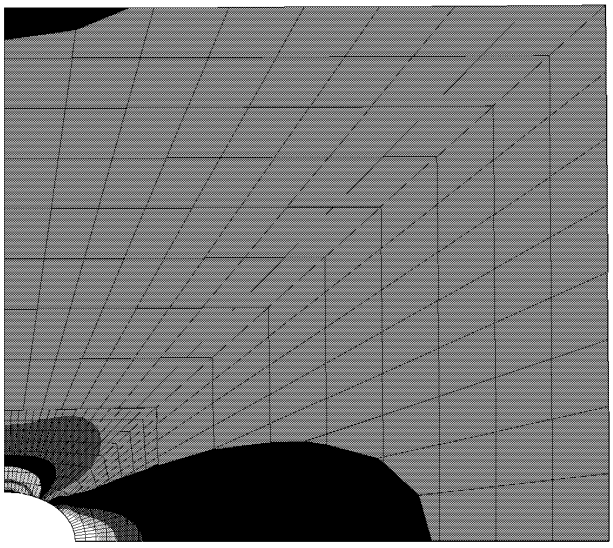

Figure 9: Horizontal Stress Contours on Deformed Shape (p=8)

The stress concentration factors at p=4 are listed in Table 5 for two conforming and one non–conforming meshes with interface elements and two conforming meshes without interface elements, which will serve as baselines. The value calculated from [8] for a semi–infinite plate is 2.72, which is derived from curve fits to photoelastic data for a specified accuracy of much less than 5%. For the two conforming configurations, the meshes with and without interface elements match exactly. The stress concentration factor for the non–conforming mesh falls slightly outside the range of the conforming configurations, but the solution at p=4 has not yet converged.

Table 5: Stress Concentration Factor (p=4)

Mesh	Stress Concentration
two/two without interface	2.933
two/two with interface	2.933
four/two with interface	2.839
four/four with interface	2.846
four/four without interface	2.846

The stress concentration factors at p=8 are listed in Table 6 for the same three meshes with interface elements and two meshes without. For the two conforming configurations, the meshes with and without interface elements match exactly. In addition, they match each other and the non–conforming mesh to the accuracy shown, since the p=8 solution has converged.

Table 6: Stress Concentration Factor (p=8)

Mesh	Stress Concentration
two/two without interface	2.778
two/two with interface	2.778
four/two with interface	2.778
four/four with interface	2.778
four/four without interface	2.778

5. Conclusions

Interface elements for dissimilar p–shell meshes along geometric curves have been implemented in MSC/NASTRAN. These elements are applicable to a wide range of problems. Applications where the analyst specifies the interface manually include facilitating global/local analysis and attaching components from different sources, and applications where the interface elements could be generated automatically are related to automeshers and h–refinement. The interface elements use the hybrid variational formulation developed by NASA, which was summarized in this paper along with the implementation in MSC/NASTRAN.

Several sets of example problems were demonstrated, ranging from simple models with exact solutions to more complicated applications for global/local analysis. The cantilever beam models showed that the interface elements provide the exact solutions, even for non–conforming meshes. They also showed that the solutions were stable as the p–level increased beyond the exact solution. The Scordelis–Lo roof showed the use of interface elements on a curved surface, where the solution has both membrane and bending components and is therefore more complex. The plate with hole model showed that the interface elements could be used efficiently for global/local analysis, using more elements in the area of interest without have to transition to the model boundaries. The local area in that model could be removed and replaced with a more refined mesh, if desired. In addition, the latter two models demonstrated that for conforming configurations, meshes with and without the interface elements provided identical results.

It is important to note that the interface elements provide a tool for connecting dissimilar meshes, but they do not increase the accuracy of the mesh. As with any interface formulation, the hybrid variational technology, which imposes continuity conditions in a weak form, can not increase the accuracy of the adjacent subdomains. For instance, if a single element edge on one boundary is connected to many element edges on the other boundary, the analysis is going to be limited to the accuracy of the less accurate subdomain, no matter how good the interface element is. This restriction should be considered when deciding how close to the areas of primary interest to put the interface elements.

6. Acknowledgement

This work was performed in conjunction with NASA Cooperative Agreement NCC1–202, ‘‘Commercialization of NASA Interface Technology,’’ signed October 18, 1994.

7. References

1. M.A. Aminpour, J.B. Ransom, and S.L. McCleary, ‘‘Coupled Analysis of Independently Modeled Finite Element Subdomains,’’ presented at the AIAA/ASME/ASCE/AHS/ASC 33rd Structures, Structural Dynamics, and Materials Conference, Dallas, Texas, April 13–15, 1992.
2. J.B. Ransom, S.L. McCleary, and M.A. Aminpour, ‘‘A New Interface Element for Connecting Independently Modeled Substructures,’’ presented at the AIAA/ASME/ASCE/AHS/ASC 34th Structures, Structural Dynamics, and Materials Conference, La Jolla, California, April 19–21, 1993.
3. M.A. Aminpour, J.B. Ransom, and S.L. McCleary, ‘‘A Coupled Analysis Method for Structures with Independently Modelled Finite Element Subdomains,’’ *International Journal for Numerical Methods in Engineering*, Vol. 38, pp. 3695–3718 (1995).
4. J.M. Housner, M.A. Aminpour, C.G. Dávila, J.E. Schiermeier, W.J. Stroud, J.B. Ransom, and R.E. Gillian, ‘‘An Interface Element for Global/Local and Substructuring Analysis,’’ presented at the MSC 1995 World Users’ Conference, Los Angeles, California, May 8–12, 1995.
5. ‘‘MSC and NASA Agreement to Include NASA Technology in MSC/NASTRAN,’’ *MSC/WORLD*, Vol. V, No. 1, pp. 23–24 (February 1995).
6. MSC/NASTRAN Quick Reference Guide Version 69, The MacNeal–Schwendler Corporation, Los Angeles, California (to be published).
7. R.H. MacNeal and R.L. Harder, ‘‘A Proposed Standard Set of Problems to Test Finite Element Accuracy,’’ *Finite Elements in Analysis and Design*, Vol. 1, pp. 3–20 (1985).
8. R.J. Roark and W.C. Young, *Formulas for Stress and Strain*, Fifth Edition, McGraw–Hill, Inc., New York (1975).